Applications of Simplified Fuzzy ARTMAP to Partial Discharge Classification and Pattern Recognition

BOONRUANG MARUNGSRI and SUPHACHAI BOONPOKE
High Voltage Insulation Technology Research Laboratory,
Alternative and Sustainable Energy Research Unit
School of Electrical Engineering, Institute of Engineering, Suranaree University of Technology
Muang District, Nakhon Ratchasima, 30000, THAILAND
Email: bmshvee@sut.ac.th

Abstract: - Artificial intelligent techniques have been widely used in high voltage insulation technology application. In this paper, the effectiveness of artificial intelligent technique to apply for pattern recognition and classification of Partial Discharge (PD) is presented. Partial discharge signal was generated and measured by using an artificial partial discharge source. Characteristics of PD signal for pattern recognition and classification were determined by using statistical and fractal methods from relationship among the voltage phase angle, the discharge magnitude and the repeated existing of partial discharges. The simplified fuzzy ARTMAP (SFAM) was used as artificial intelligent technique for pattern recognition and classification. PDs characteristic quantities were used as input parameters for Simplified Fuzzy ARTMAP to train pattern recognition and classification system. Pattern recognition and classification results were obtained. The results demonstrated the high effectiveness of the purpose technique applied for pattern recognition and classification of partial discharge.
.

Key-Words: - Partial discharges, PD Pattern recognition, PD Classification, Artificial intelligent, Simplified Fuzzy ARTMAP.

1 Introduction

Generally, partial discharge (PD) is electrical discharges that do not completely bridge the distance between two electrodes under high voltage stress. Partial discharges are small electrical sparks that occur within the imperfect insulation system of electrical apparatus. Although the magnitude of such discharges is usually small, it causes progressive deterioration and may lead to ultimate failure [1],[2].

Partial discharge is one of the factors that could lead to failure of electrical apparatus. Also, partial discharges could destroy insulation and cause ageing of insulation. Occurrence of partial discharge in electrical insulation is always associated with emission of several signals (i.e. electrical signal, acoustic pulses and chemical reactions).

Recently, artificial intelligent techniques have been widely adopted to many applications in electrical engineering field[3]–[8]. The objectives of this work are to apply an artificial intelligent technique, simplified fuzzy ARTMAP (SFAM), as well as to classify and recognize partial discharge. In this paper, classification of partial discharge is given in Section 2, detection techniques for partial discharge are given in Section 3, characteristics of partial discharge quantities are given in Section 4, and the detail of SFAM is given in Section 5. In addition, experimental results and PDs pattern recognition are illustrated in Section 6 and Section 7, respectively. Finally, discussion and conclusion are provided.

2 Classification of Partial Discharge

Basically, partial discharges are divided into four types: (i) internal discharges, (ii) corona discharges, (iii) surface discharges and (iv) discharges in electrical trees, as shown in Fig. 1 [1],[9].

2.1 Internal Discharges

Internal discharges occur in inclusions of low dielectric strength. These discharges usually occur in gas–filled cavities, but oil – filled cavities can also break down and cause gaseous discharges afterwards. Internal discharges are capable of degrading the insulation depends on the field strength, the kind of material and the discharges magnitude. (Fig. 1.a)

2.2 Corona Discharges

Corona discharges occur at sharp points in the electrical field. These discharges may occur in gases and in liquids. They occur usually at the high-voltage side, but at sharp edges at earth potential, or even at half- way the electrodes also may cause corona discharges. (Fig. 1.b)

2.3 Surface Discharges

Surface discharges may occur in gases or in oil if there is a strong stress component parallel to the dielectric surface. These discharges are known to cause deterioration of dielectrics by heating the dielectric boundary, through charges trapped in the surface and through the formation of chemicals such as nitric acid and ozone. (Fig. 1.c)

2.4 Discharges by Electrical Treeing

Electrical trees can start from defects in the solid insulation. After treeing has started a hollow stem and several branches are generated. (Fig. 1.d)

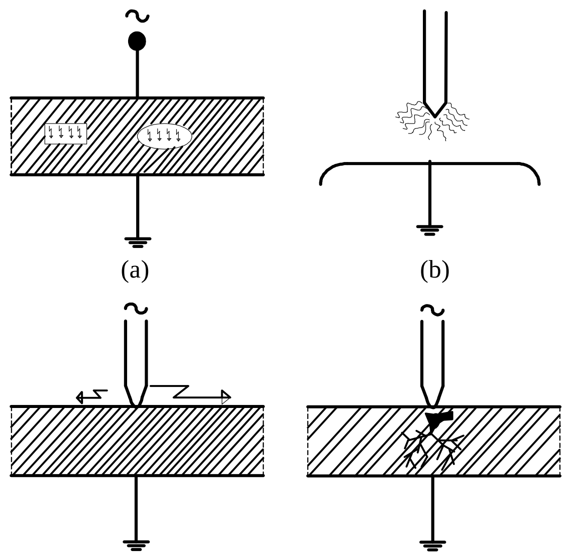

Fig. 1 Types of Partial Discharges.

3 Detection Techniques for Partial Discharge

Occurrence of PDs in electrical insulation is always associated with emission of several signal electrical signal, acoustic signal and chemical reactions, i.e. heat, sound, light and gas. The method to detection PD signal can be grouped into three categories, based on the PD manifestation that they measure: chemical, acoustic and electrical detections [9].

Chemical detection: One of the consequences of PDs is chemical change of material. (i.e. oil, solid and gas)[10].

Acoustic detection of PD is based on the detection of the mechanical waves propagated from the discharge site to the surrounding medium. Acoustic detection has been widely used in diagnostics of transformers. The primary advantage of using acoustic detection is position information is readily available from acoustic systems using sensors at multiple locations [11]-[13].

Electrical partial discharges detection methods are based on the appearance of a partial discharges pulse at the terminals of a test object. Electrical detection includes two methods: Pulse Current Method and Ultra High Frequency Method (UHF).

Pulse Current Method: This method gets the apparent charge by detecting the PD current in detecting impedance [9],[14]. Pulse Current Method is easy for quantitative measurement and it has high sensitivity.

Ultra High Frequency Method (UHF): UHF detection which is based on the detection of electrical resonance at ultrahigh frequencies can be applied to realize not only the phenomena but also the location of a PD source [15] – [17].

In this paper, electrical detection technique was adopted to measure partial discharges signal. Most partial discharges detection systems are integrated into the test circuit in accordance with the diagram shown in Fig. 2.

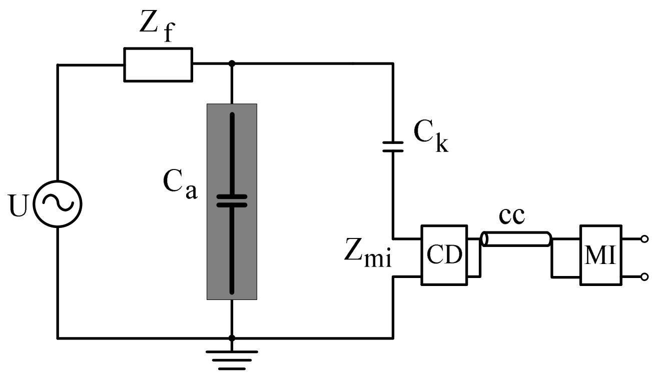

Fig. 2 Basic Partial Discharge Test Circuit

U high-voltage supply
Z_{mi} input impedance of measuring system
CC connecting cable
Ca test object
Ck coupling capacitor
CD coupling device
MI measuring instrument
Z_f filter

The coupling capacitor, C_k, shall be low of inductance design and should exhibit a sufficiently low level of partial discharges at the specified test voltage to allow the measurement of the specified partial discharge magnitude.

The high voltage power supply shall have sufficiently low level of background noise to allow the specified partial discharge magnitude to be measured at the specified test voltage.

4 Characteristics of Partial Discharge

Characteristics of partial discharges for pattern recognition and classification are computed from the relation of the voltage phase angle, the discharge magnitude and the repeated existing of partial discharges by using statistical and fractal methods [1],[9],[14].

4.1 Basic Quantities

Quantities of the first group will be termed basic quantities. For their registration, the momentary values of the test voltage and the discharge signal are registered. The electrical activity of partial discharges can be represented by two independent quantities:

(a) Discharge magnitude
(b) Discharge timing

4.2 Deduced Quantities

Quantities of the second group will be termed deduced quantities. For their registration, the basic quantities have to be observed during a time span that is much longer than the duration of one voltage cycle. These quantities can be analyzed as a function of time and a function of the phase angle.

The quantities as function of time describe the changes of the basic quantities in the course of time.

The quantities as function of the phase angle represent the recurrence of partial discharges related to their phase angle. The voltage cycle is divided into phase window representing the angle axis (0–360°). The four quantities can be determines in each phase window.

(1) The sum of the discharge magnitudes observed in one phase window (discharge amount).

(2) The number of discharges observed in one phase window (pulse count).

(3) The average value of discharges observed in one phase (mean pulse height).

(4) The maximum value of discharge observed in one phase window (maximum pulse height).

4.3 Statistical Operators

Quantities of the third group will be termed as statistical operators. They provide the analysis of the deduced quantities from the second group.

The pulse count distribution, $H_n(\varphi)$, represents the number of the observed discharges in each phase window as a function of the phase angle.

The mean pulse height distribution, $H_{qn}(\varphi)$, represents the average amplitude in each phase window as a function of the phase angle. $H_{qn}(\varphi)$ is derived from the total discharge amount in each phase window divided by the number of discharges in the same phase window.

In the case of a single defect, discharge quantities can be fairly well described by a normal distribution process. To get a better evaluation of $H_{qn}(\varphi)$ and $H_n(\varphi)$ quantities, several statistical parameters can be used. They are here termed as statistical operators. For a discrete distribution function, $f(x)$, the operators can be express as:

$$f(x) = P(X = x_i) = p_i \tag{1}$$

where P is the probability: x_i is the discrete value: p_i is the probability value for x_i. The following moments u_k of a distribution can be defined:

$$u_k = \sum (x_i - a)^k \cdot p_i \tag{2}$$

First moment: u - mean value of a distribution; k=1, a=0

$$u = \sum x_i \cdot p_i \tag{3}$$

Second moment: σ^2- variance value of a distribution; k =2, $a = u$

$$\sigma^2 = \sum (x_i - u)^2 \cdot p_i \tag{4}$$

Third moment: skewness sk - indicator of the asymmetry of a distribution as compared to a normal distribution; k=3, $a = u$

$$S_k = \sum \frac{(x_i - u)^3 \cdot p_i}{\sigma^3} \tag{5}$$

Fourth moment: kurtosis K_u - indicator of the sharpness of a distribution as compared to a normal distribution; k =4, $a = u$

$$Ku = \sum \frac{(x_i - u)^4 \cdot p_i}{\sigma^4} - 3 \tag{6}$$

The third moment and the fourth moment about the mean are significant with respect to the shape of the distribution.

The skewness,*sk*, indicates the asymmetry of the distribution. *sk* will be zero for asymmetric distribution, positive when the distribution is asymmetric to the left and negative when the distribution is asymmetric to the right.

The kurtosis, *Ku*, indicates the degree of sharpness of the distribution. Kurtosis *Ku* will be zero for a normal distribution. If the distribution is sharper than the normal distribution, *Ku* is positive while if that is flatter than the normal distribution, *Ku* is negative.

The discharges during a voltage cycle occur in two sequences. For each half of the voltage cycle separate discharge patterns can be found. Thus, the $H_{qn}(\varphi)$ and $H_n(\varphi)$ quantities are characterized by two distributions. For the positive half of the voltage cycle $H^+_{qn}(\varphi)$, $H^+_n(\varphi)$ and for the negative half of the voltage cycle $H^-_{qn}(\varphi)$, $H^-_n(\varphi)$.

Both the $H_{qn}(\varphi)$ and $H_n(\varphi)$ quantities can be described by two skewness, Sk^+, Sk^-, and two kurtosis Ku^+, Ku^-. The distributions $H_{qn}(\varphi)$ and $H_n(\varphi)$ are also characterized by their mean value, their inception phase and the number of peaks. Therefore more statistical parameters can be defined, enabling us to compare the mean value, the inception phase and the number of peaks in the both positive and the negative half of the voltage cycle. The distributions $H_{qn}(\varphi)$ and $H_n(\varphi)$ both positive and negative half of the voltage cycle the following statistical operators have been introduced by discharge asymmetry, Q , as the quotient of the mean discharge level in the positive and in the negative half of the voltage cycle.

$$Q = \frac{Q_s^- / N_q^-}{Q_s^+ / N_q^+} \tag{7}$$

The cross-correlation factor, *cc*, can be expressed as:

$$cc = \frac{\sum x_i y_i - \sum x_i \sum y_i / n}{\sqrt{\left[\sum x_i^2 - (\sum x_i)^2 / n\right]\left[\sum y_i^2 - (\sum y_i)^2 / n\right]}} \tag{8}$$

The modified cross-correlation factor, *mcc*, which is used to evaluate the difference between discharge patterns in the positive and the negative half of the voltage cycle is given in (9).

$$mcc = Q \cdot cc \tag{9}$$

5 Simplified Fuzzy ARTMAP

In 1976, Adaptive Resonance Theory (ART) was invented by Grossberg, as a theory of human cognitive information processing [18]. Carpenter and Grossberg introduced the ART family in the form of a wide variety of supervised and unsupervised NNs [19]–[22]. The most advanced model of the ART family, fuzzy ARTMAP (FAM), could handle both binary and analogue data in a supervised manner [23]. The main drawback to the ART family networks, which prevented others from using them, was their intricacy: the inventors had introduced complicated architectures for their networks instead of presenting them as simple algorithms. This problem later was recognized by the inventors and they presented the modified model or simplified model of ART family networks [24].

Originally, ART networks were defined in terms of differential equations, but in practice they are implemented using approximations or analytical solutions to these equations, in the limit. ART networks have their own special terminology. The main idea of unsupervised ART networks is as follows:

(1) Find the nearest cluster prototype that 'resonates' with the input pattern.

(2) Update this cluster prototype to be closer to the input.

Kasuba have been developed simplified fuzzy ARTMAP (SFAM) and details are illustrated in [24]. Kasuba's Simplified fuzzy ARTMAP which is a vast simplification of Carpenter and Grossberg's fuzzy ARTMAP has reduced computational overhead and architectural redundancy when compared to its predecessor. Also, the model employs simple learning equations with a single user selectable parameter and can learn every single training pattern within a small number of training iterations. So, the SFAM is much faster than the FAM and easier to understand and simulate. However, it should be made clear that the SFAM can be used only for classification. The SFAM consists of a two layer net containing an input and an output layer. Figure 3 illustrates the architecture of simplified fuzzy ARTMAP.

The main idea of SFAM is as follows[25]:

(1) Find the nearest subclass prototype that 'resonates' with the input pattern (winner).

(2) If the labels of the subclass and the input pattern match, update the prototype to be closer to the input pattern.

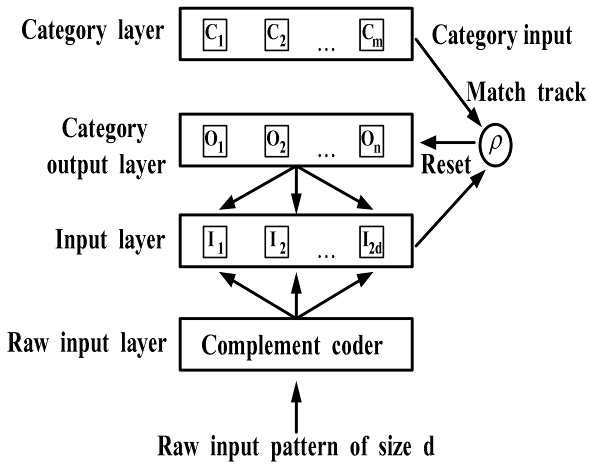

Fig. 3 Architecture of SFAM Network

(3) Otherwise, reset the winner, temporarily increase the resonance threshold (r), and try the next winner.

(4) If the winner is uncommitted, create a new subclass (assign the input vector to be the prototype pattern of the winner, and label it as the class label of the input).

The input to the network flows through the complement coder where the input string is stretched to double the size by adding its complement also. The complement codes input then flows into the input layer and remains there. Weights (*w*) from each of the output category nodes flow down to the input layer. The category layer merely holds the names of the *M* number of categories that the network has to learn. Vigilance parameter and match tracking are mechanisms of the network architecture which are primarily employed for network training.

ρ is the vigilance parameter which can range from 0 to 1. It controls the granularity of the output node encoding. Thus, while high vigilance values make the output node much fussier during pattern encoding, low vigilance renders the output node to be liberal during the encoding of patterns.

The match tracking mechanism of the network is responsible for the adjustment of vigilance values. Thus, an error occurs in the training phase during the classification of patterns.

The SFAM algorithm is as follows [25]:

Step 1: Set the vigilance factor to be equal to its baseline value :

$$\rho = \overline{\rho} \tag{10}$$

Step 2: Insert input, and calculate second layer activities:

$$T_j(I) = \frac{|I \wedge w_j|}{\alpha + |w_j|} \quad \text{for } j = 1,\ldots, N\text{-}19 \tag{11}$$

and for the uncommitted neuron: $T_N = T_0$

Step 3: Find the winner

$$J = arg\begin{bmatrix} Max(T_j) \\ j \end{bmatrix} \tag{12}$$

If the winner neuron is uncommitted, go to **Step 7**.

Step 4: Check the resonance condition, i.e. if the input is similar enough to the winner's prototype:

$$\frac{|I \wedge w_j|}{|I|} = \frac{|I \wedge w_j|}{M} \geq \rho \tag{13}$$

If this condition is fulfilled, go to **Step 5**.

If this condition is not fulfilled, reset the winner (T_j = -1), go to the **Step 3**, and check the next winner.

Step 5: If the class label of the winner matches with the class label of input, update the prototype pattern to be closer to the input pattern:

$$w_j^{(new)} = \beta(I \wedge w_j^{(old)}) + (1-\beta)w_j^{(old)} \tag{14}$$

and go to **Step 9**, otherwise reset the winner (T_j = -1), temporarily increase the vigilance factor so as to violate the condition of Equation (9), i.e. set ρ equal to :

$$\rho = \frac{|I \wedge w_j|}{M} + \varepsilon \tag{15}$$

(where ε is a small positive number, i.e. $\varepsilon \approx 0.001$).

Step 6: If $\rho > 1$, terminate the training for this input pattern in the current epoch (data mismatch), and go to **Step 9**, otherwise go to **Step 3**, and try the next winner.

Step 7: Create a new subclass, i.e. assign the input vector as the prototype pattern of the winner neuron:

$$w_N = I \tag{16}$$

and set the class label of the winner neuron to be as the class label of input pattern.

Step 8: Create a new uncommitted neuron, and: $N \leftarrow N + 1$.

Step 9: Go to the **Step 1,** and repeat the algorithm for the next input.

The flow chart of the SFAM Algorithm is presented in Fig. 4.

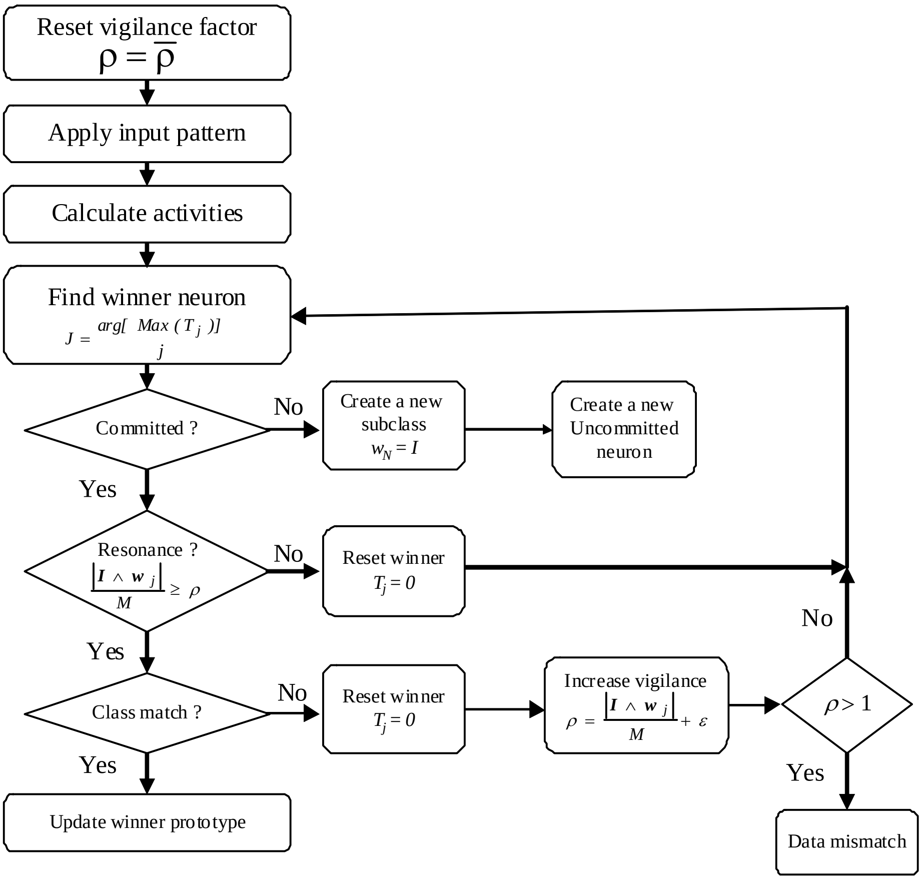

Fig. 4 Flow Chart of the SFAM Training Algorithm for One Input Pattern in One Epoch of Training

Once the network has been trained, the inference of pattern, known or unknown, i.e. the categories to which the pattern belongs, may be easily computed. This is accomplished by passing the input pattern into the complement coder and then to the input layer. All the output nodes compute the activation functions with respect to the input. The winner, which is the node with the highest activation function, is chosen. The category to which the winning output node belongs is the one to which the given input pattern is classified by the network. The overall structure of the pattern recognizer is illustrated in Fig. 5.

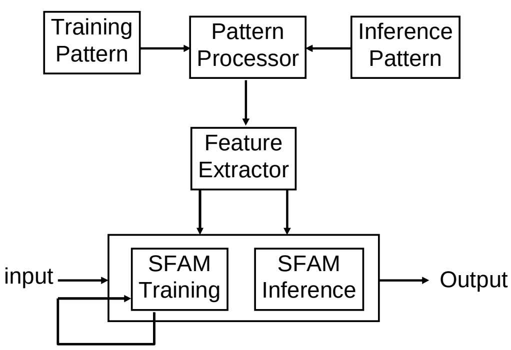

Fig. 5 Structure of SFAM based pattern recognizer

The SFAM activator functions as two modules, namely the training module and the interference module.

Steps of SFAM algorithm for the training phase are as follows[26].

Step 1: Choose an appropriate value for the vigilance parameter ($0 \leq \rho < 1$) and a small value for α. Set *NO_OF_TRAINING_EPOCHS* to the desired number of training epochs and *COUNT_OF TRAINING_EPOCHS* to 0.

Step 2: $i \leftarrow 1$;

COUNT_OF_TRAINING_EPOCHS = *COUNT_OF _TRAINING_EPOCHS*+1; while (*COUNT_OF_TRAINING _EPOCHS* ≤ *NO_OF_ TRAINING_EPOCHS*)

Repeat **Steps 3–12**;

Step 3: Input the pattern vector $I_i = (a_{i1}, a_{i2}, \ldots a_{id})$ of dimension d and its category C_i.

Step 4: Compute the augmented input vector

$$AI_i = (a_{i1}, a_{i2}, \ldots, a_{id}, 1 - a_{i1}, 1 - a_{i2}, \ldots, 1 - a_{id})$$

Step 5: If AI_i is the first input in the given category C_i set the top down weight vector W_j as AI_i

i.e. $W_j = AI_i$

Link W_j to the category C_i;

Go to **Step 12**;

Step 6: If AI_i is an input pattern vector whose category already exists then compute the activation function

$T_j(AI_j)$ for each of the existing top-down weight nodes W_j

$$T_j(AI_i) = \frac{|AI_j \wedge W_j|}{\alpha + |W_j|};$$

Step 7: Choose that top-down weight node k which records the highest activation function

$$T_k(AI_i) = \max_j T_j(AI_i)$$

Step 8: Compute the match function $MF_k(AI_i)$ of the winning node k;

If $MF_k(AI_i) > \rho$ and C_i is same as that category C_k linked to W_k

Then update weight vector

$$W_k \text{ as } W_k^{new} = W_k^{old} + (I \wedge W_k^{old})$$

(Here $\beta = 1$ has been chosen in Eq.8)

Go to **Step 12**;

Step 9: If $MF_k(AI_i) > \rho$ and C_i is not the category C_k linked to W_k then

Undertake match tracking by setting ρ to $MF_k(AI_i)$ and incrementing by a small value ε.

$$\rho = MF_k(AI_i) + \varepsilon \; ;$$

If some more top-down weight nodes exist

Then consider the next highest winner W_k among the top-down weight nodes;

Go to **Step 8**;

Else go to **Step 11**;

Step 10: If $MF_k(AI_i) > \rho$

Then

If some more top-down weight nodes exists

Then

Consider the next highest winner W_k among the top-down weight nodes.

Go to **Step 8**;

Else go to **Step 11**;

Step 11: Create a new top-down weight node W_1 such that $W_1 = AI_i$ and link the node to the category C_i;

Step 12: If no more input pattern then go to **Step 13**;

Else $i \leftarrow i+1$

Go to **Step 3**;

Step 13: Go to **Step 2**;

END SFAM –TRAIN.

Steps of SFAM algorithm for the inference phase are as follows[26].

Step 1 : Let W_j , j = 1,2,3…s indicate s top-down weight vectors obtained after training the network with a given set of training patterns;

Let I_i be the inference pattern set each of whose category is to be inferred by the network; $i \leftarrow 1$;

Step 2 : Read input I_i;

Step 3 : Compute the augmented input AI_i;

Step 4 : For $j \leftarrow 1$ to s

Compute the activation functions

$$T_j(AI_i) = \frac{|AI_i \wedge W_j|}{\alpha + |W_j|}$$

End

Step 5 : Choose the winner k among the s activation functions

$$T_k(AI_i) = \max_j T_j(AI_i)$$

Step 6 : Output the category C_k linked to $T_k(AI_i)$ as the one to which I_i belongs to.

Step 7 : If no more inference pattern vectors

Then exit

Else $i \leftarrow i+1$;

Go to **Step 2**;

END SFAM-INFERENCE.

As illustrated in Fig. 5, the feature vectors of the training patterns and the categories to which they belong are presented to the SFAM's training module. The only selectable parameter for the training session is the vigilance parameter, ρ, where 0 < ρ <1. Once the training is complete, the top-down weight vectors represent the pattern learnt. Next, the feature vectors are recognized/classified and are presented to the interference module. The SFAM now begins its classification of input data by associating the feature vectors with the top-down weight vector.

6 Experimental

In this study, test arrangement is shown in Fig. 6. as illustrated in Fig 7, three types of partial discharge generation sources, including corona discharge, surface discharge and internal discharge, were used. Partial discharge signal was measured by using partial discharge detector (OMICRON, model MPD600). Typical measurement results of each partial discharge generation source are illustrated in Fig. 8, Fig. 9 and Fig. 10, respectively.

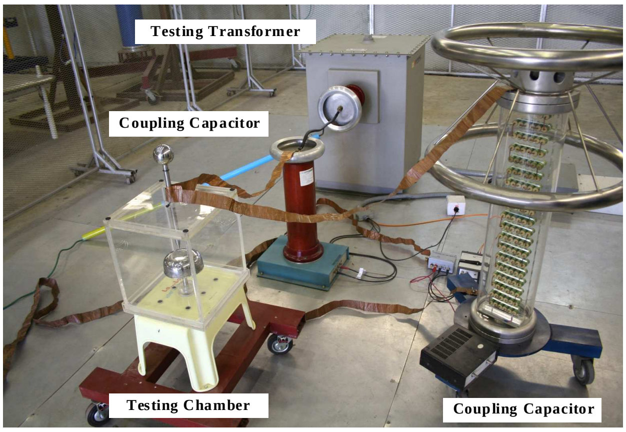

Fig. 6 Test Arrangement

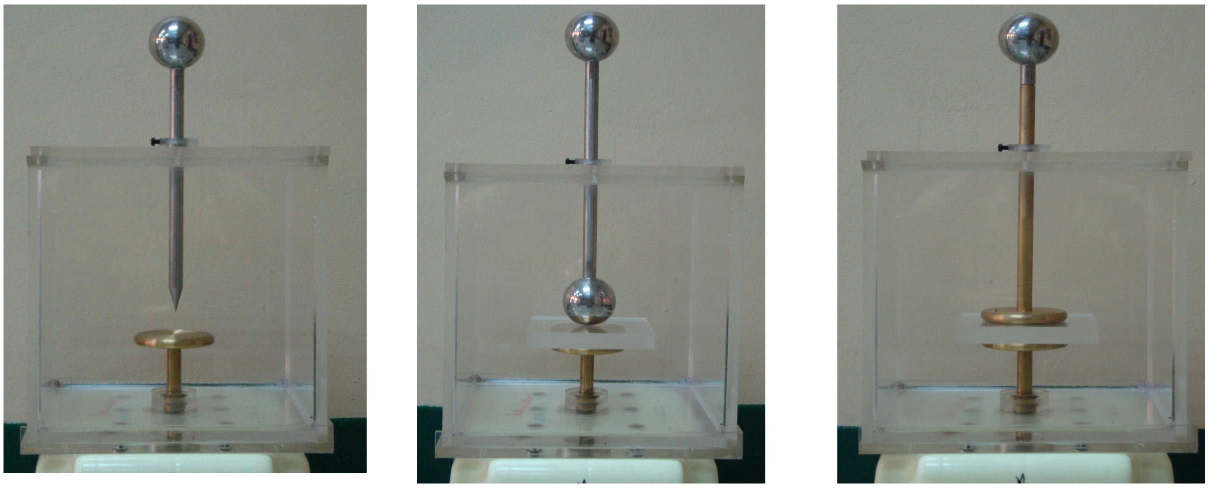

(a) Corona Discharge (b) Surface Discharge (c) Internal Discharge

Fig. 7 Electrode Configuration for Partial Discharge Generation Source

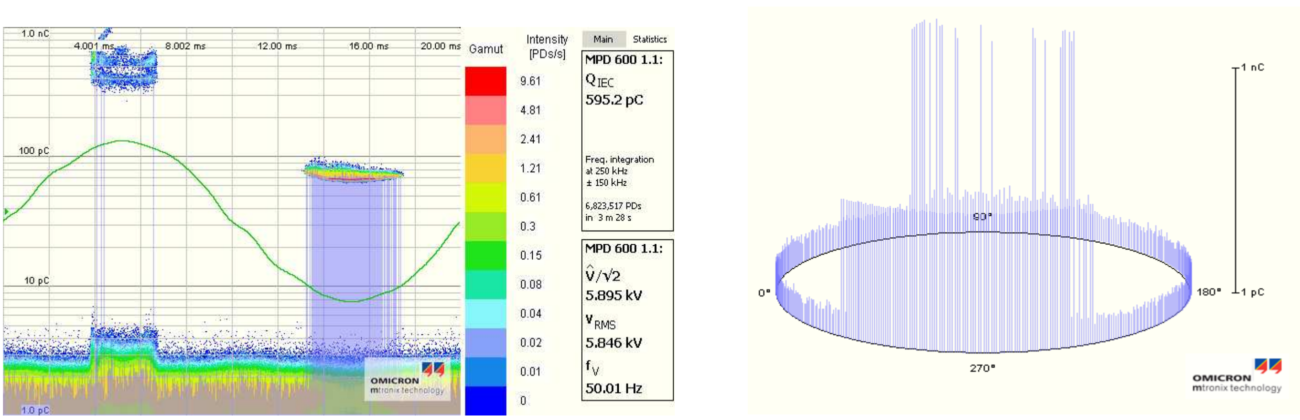

(a) Display on Sinusoidal (b) Display on Elliptical

Fig. 8 Partial Discharge Measurement Result from Corona Discharge

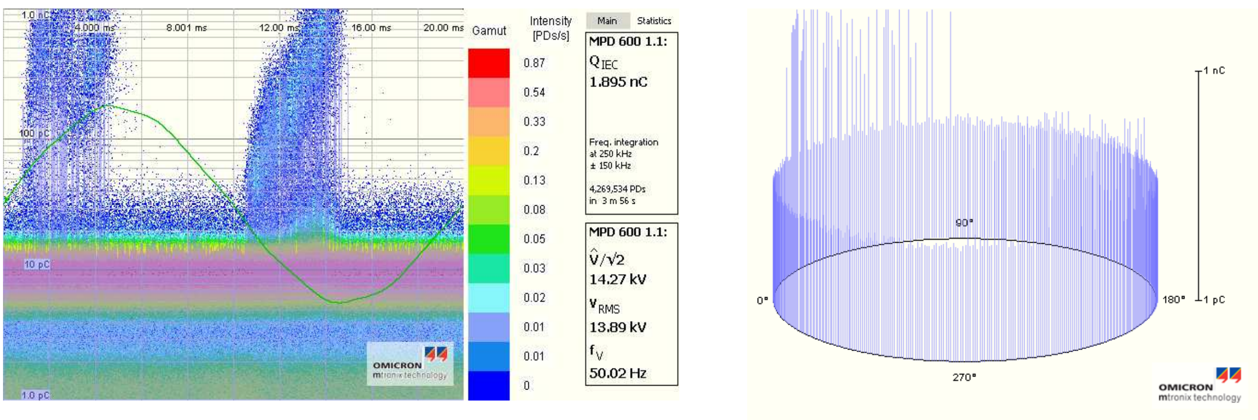

(a) Display on Sinusoidal (b) Display on Elliptical

Fig. 9 Partial Discharge Measurement Result from Surface Discharge

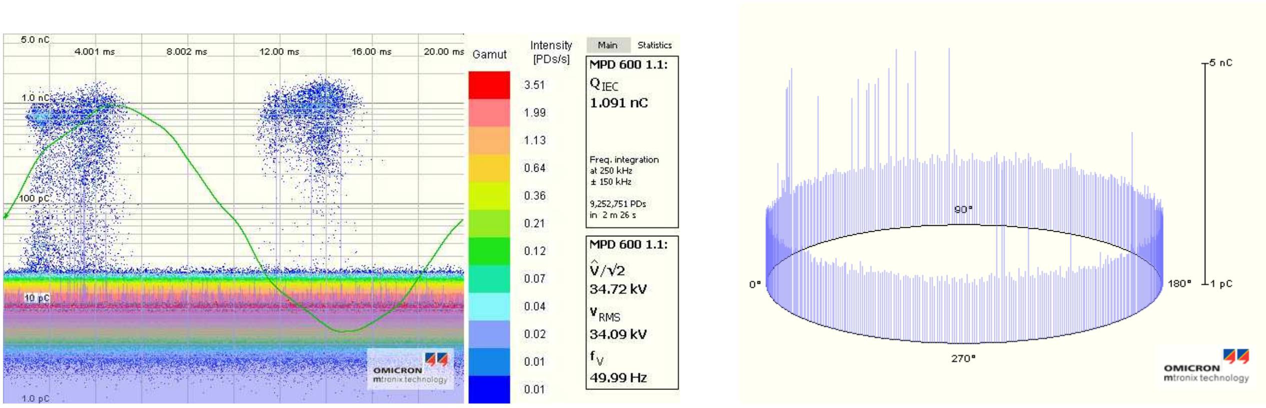

(a) Display on Sinusoidal (b) Display on Elliptical

Fig. 10 Partial Discharge Measurement Result from Internal Discharge

Obviously, differences in the pattern of partial discharge measurement results were obtained. Each partial discharge generation source generated individual partial discharge pattern. Then, these measurement data are used to test the purpose technique. Characteristics of partial discharge data were calculated by using statistical tools to apply for pattern recognition and classification. These characteristic of partial discharges include skewness, kurtosis, discharge asymmetry, the cross-correlation factor and modified cross-correlation factor. Characteristics of corona discharge, surface discharge and internal discharge are showed in Table 1, Table 2 and Table 3, respectively. These results were used for pattern recognition and classification.

Table 1 Characteristics of Corona Discharge

No.	H_{qn}				H_n			
	Sk+	*Sk-*	*Ku+*	*Ku-*	*Sk+*	*Sk-*	*Ku+*	*Ku-*
1	1.150	1.010	-1.680	-1.946	1.156	1.129	-1.710	-1.884
2	1.034	1.022	-1.514	-1.953	1.120	1.092	-1.455	-1.781
3	1.061	1.012	-1.950	-1.970	1.108	0.089	-1.638	-2.331

Table 2 Characteristics of Surface Discharge

No.	H_{qn}				H_n			
	Sk+	*Sk-*	*Ku+*	*Ku-*	*Sk+*	*Sk-*	*Ku+*	*Ku-*
1	1.525	1.473	-0.390	-0.840	1.976	-0.120	1.597	-2.070
2	1.511	1.302	-0.570	-0.560	1.977	-0.690	1.923	-2.390
3	1.459	1.302	-0.400	-1.000	1.945	-0.630	1.647	-2.360

Table 3 Characteristics of Internal Discharge

No.	H_{qn}				H_n			
	Sk+	*Sk-*	*Ku+*	*Ku-*	*Sk+*	*Sk-*	*Ku+*	*Ku-*
1	1.206	1.200	-1.470	-1.490	1.307	-0.220	-0.960	-2.38
2	1.170	1.154	-1.570	-1.610	1.168	-0.680	-1.560	-2.33
3	1.142	1.100	-1.630	-1.750	1.125	0.500	-1.640	-2.370

The existing characteristics of the partial discharge signal, illustrated in [4], were used as reference database to train the simplified fuzzy ARTMAP system. Characteristics of reference partial discharge measurement signal (corona discharges, surface discharges and internal discharges) are illustrated in Table 4, Table 5 and Table 6, respectively.

Table 4 Characteristics of Corona Discharge

No.	H_{qn}				H_n			
	Sk+	*Sk-*	*Ku+*	*Ku-*	*Sk+*	*Sk-*	*Ku+*	*Ku-*
1	1.031	1.018	-1.92	-1.95	1.077	0.947	-1.8	2.08
2	1.031	10.15	-1.92	-1.96	1.089	1.012	-1.77	-1.9
3	1.028	1.006	-1.93	-1.98	1.062	0.951	-1.84	-0.72

Table 5 Characteristics of Surface Discharge

No.	H_{qn}				H_n			
	Sk+	*Sk-*	*Ku+*	*Ku-*	*Sk+*	*Sk-*	*Ku+*	*Ku-*
1	1.493	1.471	-0.26	-0.28	1.918	-0.46	1.451	-2.3
2	1.496	1.45	-0.27	-0.39	1.954	-0.59	1.702	-2.35
3	1.486	1.454	-0.34	-0.41	1.919	-0.54	1.408	-2.35

Table 6 Characteristics of Internal Discharge

No.	H_{qn}				H_n			
	Sk+	*Sk-*	*Ku+*	*Ku-*	*Sk+*	*Sk-*	*Ku+*	*Ku-*
1	1.115	1.153	-1.71	-1.6	1.11	-0.37	-1.73	-2.39
2	1.141	1.152	-1.63	-1.6	1.113	-0.43	-1.71	-2.39
3	1.133	1.153	-1.66	-1.58	1.124	-0.63	-1.68	-2.34

7 Results and Discussions

After well training the simplified fuzzy ARTMAP system by our reference PD characteristics, then PD characteristics from the experimental results were inputted to the SFAM system for a classified partial discharge generation source. The obtaining results confirmed the effectiveness of the purpose technique. The SFAM could correctly recognize and classify partial discharge generation source from PD measurement signal characteristics. The results are showed in Table 7.

Table 7 Classification Results by the SFAM System

No. of Test Data	PD Generation Source	Results of Classification
1	corona	correct
2	corona	correct
3	corona	correct
4	surface	correct
5	surface	correct
6	surface	correct
7	internal	correct
8	internal	correct
9	internal	correct

8 Conclusions

The experimental for PD measurement was conducted. Differences in PD generation source were used in order to characterize the partial discharge measurement signal. Characteristics of PD signal were analyzed by using statistical tools and were used to classify PD generation source using the SFAM system. Correctly classification results were obtained. Moreover, it is clear that the simplified fuzzy ARTMAP system can be applied for the pattern recognition and classification of PD generation signal.

Acknowledgement

The authors would like to thank the high voltage laboratory, Department of Electrical Engineering, Faculty of Engineer, King Mongkut's Institute of Technology, Ladkrabang, Bangkok, Thailand for kindness experimental supported. The authors would like to thank Dr. Sudkhet Pojprapai for his kindness grammatical revise.

References:

[1] F.H. Kreuger, "*Partial Discharge Detection in High – Voltage Equipment*", Butterworth & Co. (Publishers) Ltd, 1989.

[2] E. Kuffel, W.S. Zaengl and J. Kuffel, "*High Voltage Engineering: Fundamentals*". 2nd, Butterworth – Heinemann, 2000.

[3] B. Marungsri, N. Meeboom and A. Oonsivilai, "Dynamic Model Identification of Induction Motors using Intelligent Search Techniques with taking Core Loss into Account", *WSEAS TRANSACTIONS on POWER SYSTEMS*, Vol. 1, No. 8, August 2006, pp. 1438 – 1445.

[4] A. Oonsivilai and B. Marungsri, "Optimal PID Tuning for AGC system using Adaptive Tabu Search", *Proceedings of the 7th WSEAS International Conference on POWER SYSTEMS*, Beijing, China, September 2007, pp. 42-47.

[5] A. Oonsivilai and B. Marungsri, "Stability Enhancement for Multi-machine Power System by Optimal PID Tuning of Power System Stabilizer using Particle Swarm Optimization", *WSEAS TRANSACTIONS on POWER SYSTEMS*, Issue 5, Volume 3, May 2008, pp. 465 – 474.

[6] A. Oonsivilai and B. Marungsri, "Optimal PID Tuning for Power System Stabilizers Using Adaptive Particle Swarm Optimization Technique", *International Conference on Power Control and Optimization: Innovation in Power Control for Optimal Industry. AIP Conference Proceedings*, Volume 1052, July 2008, pp. 116-123

[7] B. Marungsri and A. Oonsivilai, "Partial Discharges Localization in Oil Insulating Transformer using Adaptive Tabu Search", *Proceedings of the 12th WSEAS International Conference on CIRCUITS*, Heraklion, Greece, July 22-24, 2008, pp. 290 – 295.

[8] B. Marungsri and A. Oonsivilai , "Fuzzy ARTMAP Technique for Speech Noise Reduction," *WSEAS International Conference on Signal, Speech and Image Processing*, Beijing, China, pp 20-25, September 2007.

[9] E. Gulski, Computer – Aided Recognition of Partial Discharges using Statistical Tools. Delft University Press,1991.

[10] N.A. Muhamad, B.T. Phung and T.R. Blackburn, "Dissolved Gas Analysis (DGA) of Partial Discharge Fault in Bio-degradable Transformer Insulation Oil", *Universities Power Engineering Conference 2007*.AUPEC 2007, December 2007, pp 1-6.

[11] X. Wang, B. Li, H. T. Roman, O. L. Russo, K. Chin and K. R. Farmer, "Acousto– optical PD Detection for Transformers", *IEEE Transactions on Power Delivery*, Vol. 21, No. 3, July 2006, pp. 1068-1073.

[12] A. Oonsivilai and B. Marungsri, "Application of Artificial Intelligent Technique for Partial Discharges in Oil Insulating Transformer", *WSEAS TRANSACTIONS on SYSTEMS*, Vol.7 No.10, October 2008, pp.920-929.

[13] Y. Lu, X. Tan and X. Hu, "PD detection and localization by acoustic measurements in an oil-filled transformer", *IEEE Science Measurement and Technology*, Vol.147, No.2, March 2000, pp. 81-85.

[14] K. Vicetjindavat, "Pattern Recognition of Partial discharge in High Voltage Equipment", Master Degree Thesis, Chulalongkorn University, 2001.

[15] A. Wichmann, P. Grünewald, and J. Weidner, "Early fault detection inelectrical machines by on-line RF monitoring," *Cigré Symp.*, Vienna,Austria, 1987, pp. 05–87.

[16] J. T. Phillipson, "Experience with RF techniques in the petrochemical industry," *Proc. 4th Int. Conf. Generator and Motor Partial Discharge Testing*, Houston, TX, 1996.

[17] M. D. Judd, L. Yang, and I. B. B. Hunter, "Partial discharge monitoring for power transformers using UHF sensors. Part 1: Sensors and signal interpretation," *IEEE Electr. Insul. Mag.*, Vol. 21, No. 1, Mar./Apr. 2005, pp. 5-14.

[18] S. Grossberg, "Adaptive pattern classification and universal recoding, II: feedback, expectation,olfaction and illusions", *Biological Cybernetics*, Vol. 23, 1976, pp. 187–202.

[19] G. A. Carpenter and S. Grossberg, "ART2: Self-organization of stable category recognition codes for analog input patterns", *Applied Optics*, vol. 26, No. 23, 1987, pp. 4919– 4930.

[20] G. A. Carpenter and S. Grossberg, "ART3: Hierarchical search using chemical transmitters in self-organizing pattern recognition architecture, *Neural Networks*, Vol.3, 1990, pp. 129–152.

[21] G. A. Carpenter, G. S. Grossberg and J. H.Reynolds, "ARTMAP: Supervised real-time learning and classification of mon-stationary data by a self-organizing neural network", *Neural Networks*, Vol. 4, 1991, pp. 565–588.

[22] G. A. Carpenter, G. S. Grossberg and D. B. Rosen, "Fuzzy ART: Fast stable learning and categorization of analog patterns by an adaptive resonance system", *Neural Networks*, Vol. 4, 1991, pp. 759–771.

[23] G. A. Carpenter, S. Grossberg, N. Markuzon, J. H. Reynolds, and D. B. Rosen, "Fuzzy ARTMAP: A neural network architecture for incremental supervised learning of analog

multidimensional maps", *IEEE Trans. on Neural Networks*, Vol.3, No. 5, 1992, pp. 698–713.
[24] T. Kasuba, "Simplified Fuzzy ARTMAP", *AI Expert*, Vol. 8, No. 11, 1993, pp.18–25.
[25] M. Vakil-Gahimisheh and N. Pavešić, "A Fast Simplified Fuzzy ARTMAP Network", *Neural Processing Letters*, Vol. 17, 2003, pp. 273–316.
[26] S. Rajasekaran and G.A. Vijayalakshmi Pai, "*Neural networks, fuzzy logic and genetic algorithms : synthesis and applications*", New Delhi : Prentice Hall, 2006.